

Supplementary information, Figure S1

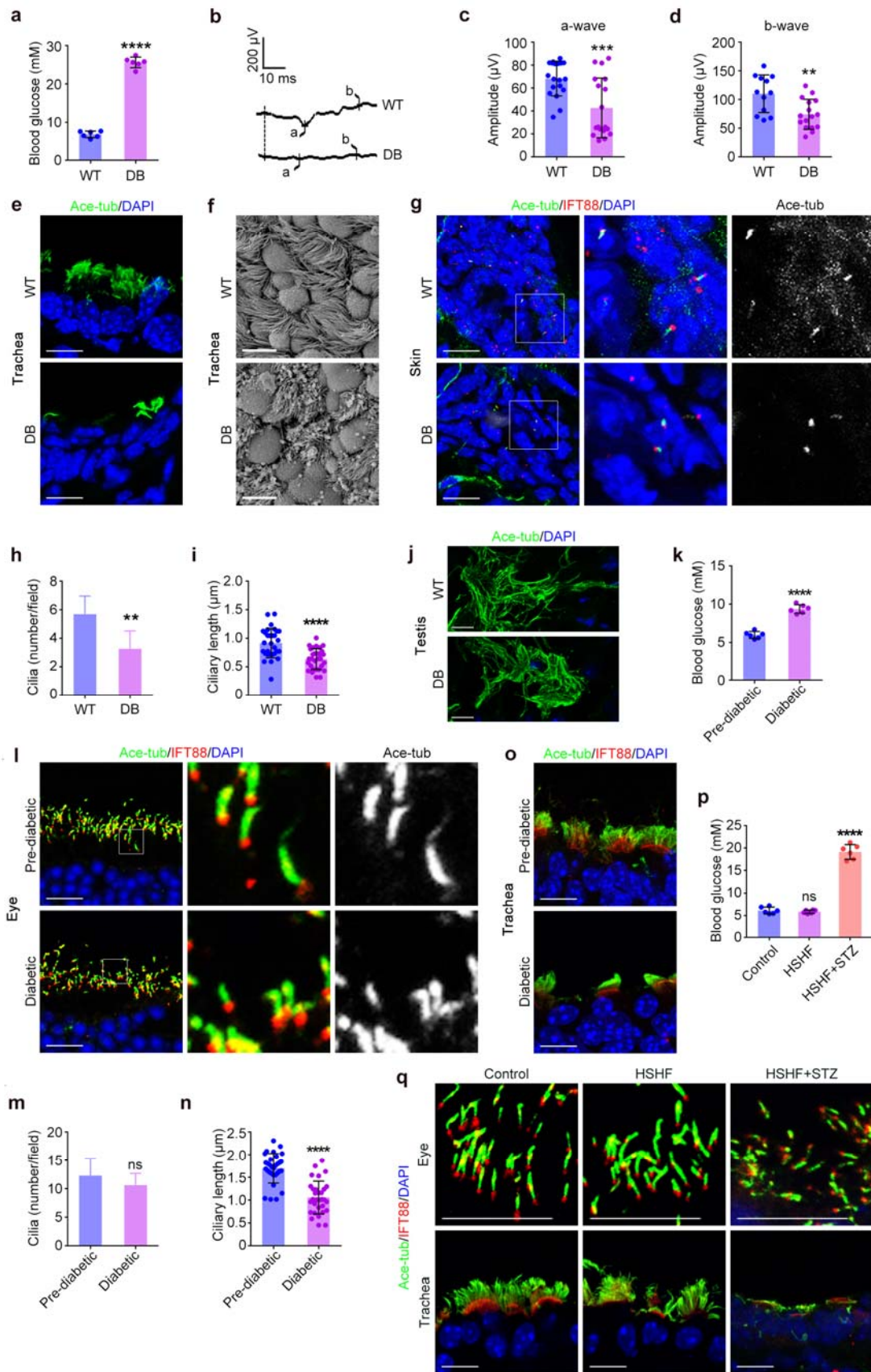


Fig. S1 Diabetic mice have ciliary defects. **a** Blood glucose levels of WT and DB mice (n = 6). **b-d** Examination of WT and DB mouse eyes with electroretinography. **e-j** Tracheal, skin, and testis tissues from WT and DB mice were subjected to immunofluorescence microscopy (**e, g, j**) or scanning electron microscopy (**f**). Ciliary density (**h**, n = 10) and length (**i**, n = 30) in skin were quantified. **k** Blood glucose levels of pre-diabetic and diabetic NOD mice (n = 6). **l-n** Eyes from pre-diabetic and diabetic NOD mice were subjected to immunofluorescence microscopy (**l**). Ciliary density (**m**, n = 10) and length (**n**, n = 30) were quantified. **o** Tracheal tissues from pre-diabetic and diabetic NOD mice were subjected to immunofluorescence microscopy. **p, q** Blood glucose levels (**p**, n = 6) and immunofluorescence images (**q**) of mouse eye and tracheal tissues. Mice were fed a high-sugar high-fat diet (HSHF) and then untreated or treated with STZ. In the control group, mice were fed a normal diet and untreated with STZ. Scale bars, 10 μ m. **P < 0.01, ***P < 0.001, ****P < 0.0001; ns, not significant. Error bars indicate SEM.

Supplementary information, Figure S2

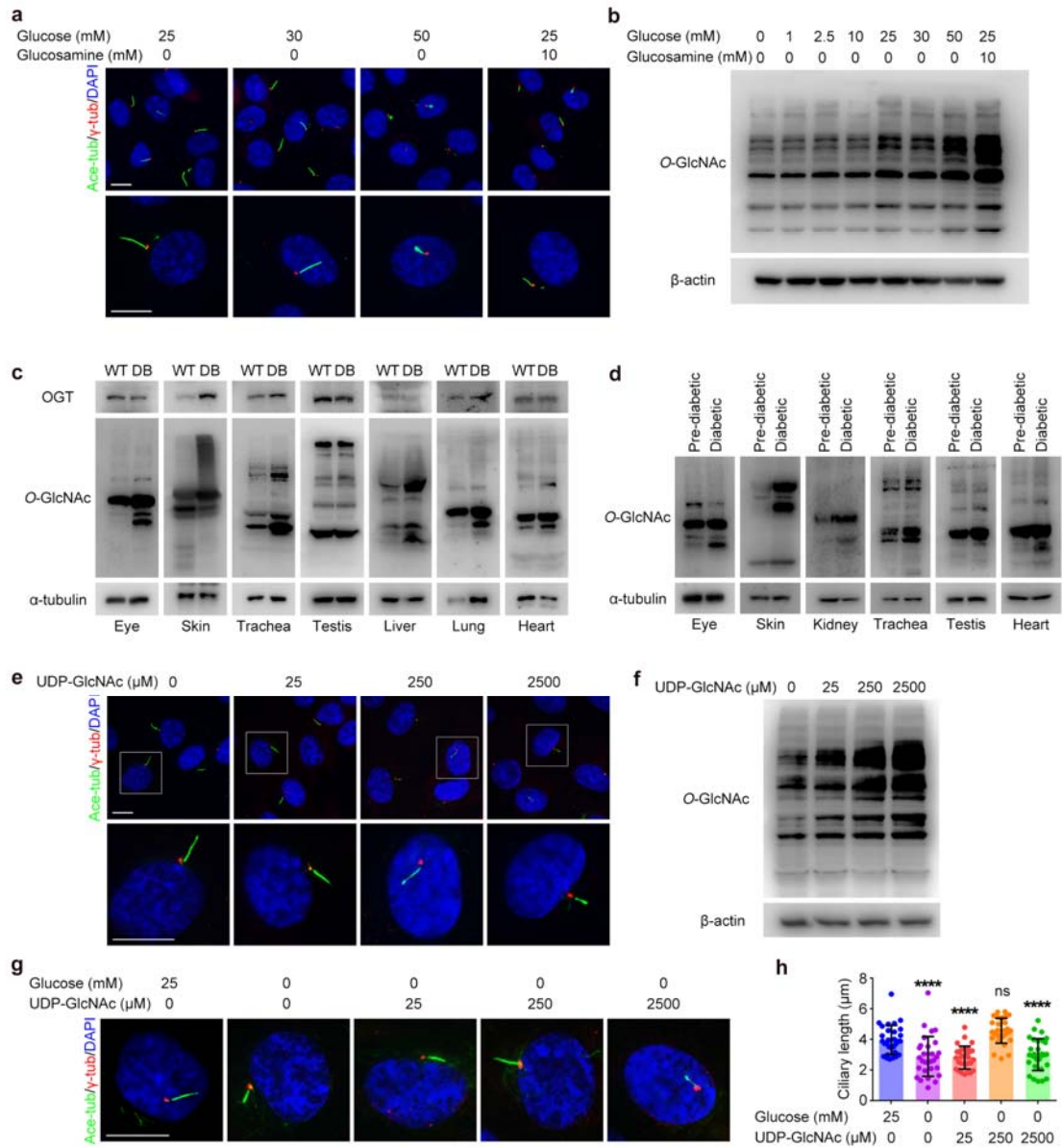


Fig. S2 Ciliogenesis is impaired by high glucose concentrations or high *O*-GlcNAcylation levels. **a, b** RPE-1 cells cultured in media containing the indicated concentrations of glucose and glucosamine were serum-starved for 48 hr. Cells were then subjected to immunofluorescence microscopy (**a**) or immunoblotting (**b**). **c** WT and DB mouse tissues were subjected to immunoblotting. **d** Tissues from pre-diabetic and diabetic NOD mice were subjected to immunoblotting. **e, f** RPE-1 cells cultured in media containing the indicated concentrations of UDP-GlcNAc were serum-starved for 48 hr. Cells were then subjected to immunofluorescence microscopy (**e**) or immunoblotting (**f**). **g, h** RPE-1 cells were cultured in serum-free medium containing the indicated concentrations of glucose or UDP-GlcNAc and subjected to immunofluorescence microscopy (**g**). Ciliary length was then quantified (**h**, $n = 30$). Scale bars, 10 μm . **** $P < 0.0001$; ns, not significant. Error bars indicate SEM.

Supplementary information, Figure S3

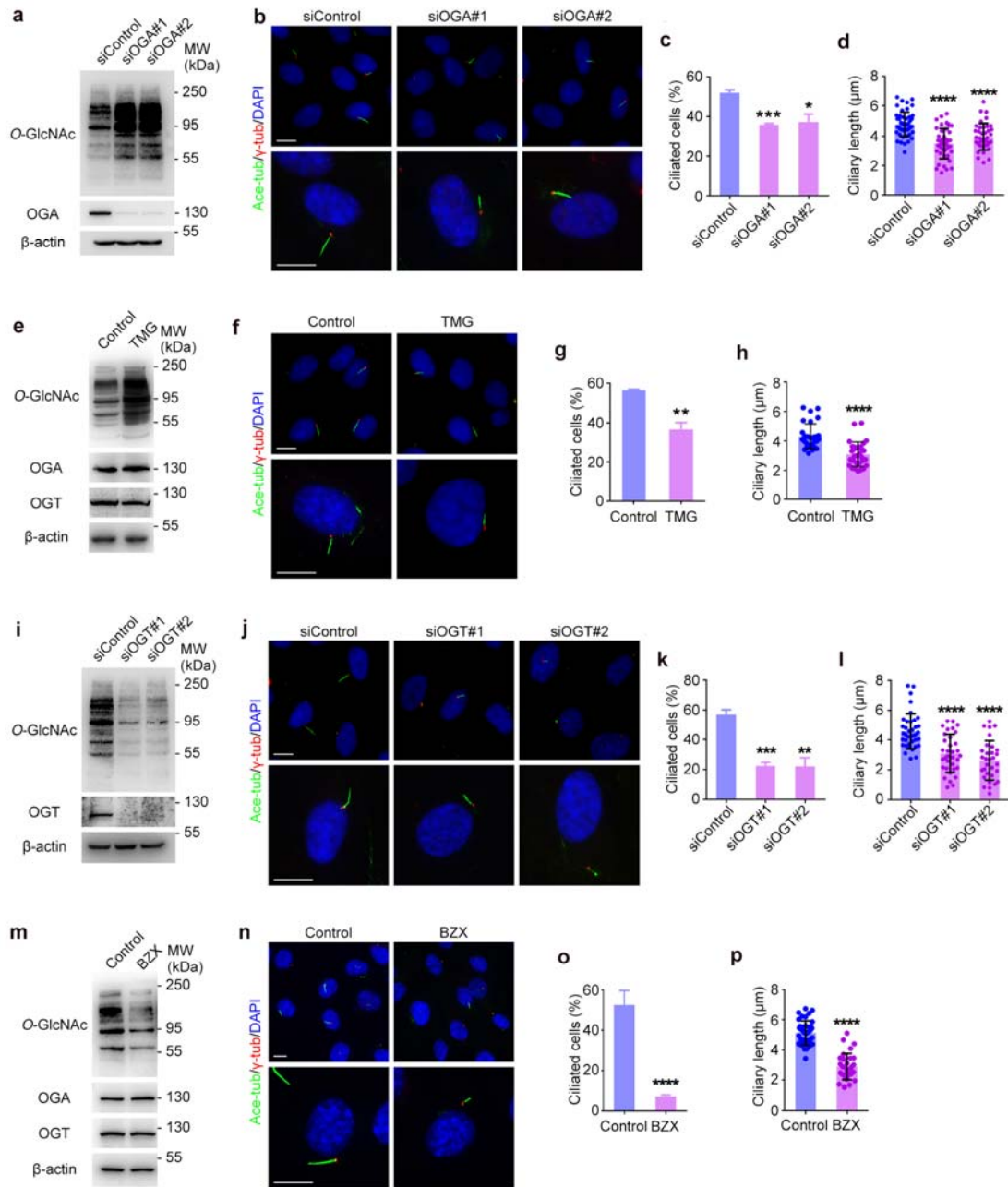


Fig. S3 Inhibition or knockdown of either OGA or OGT results in ciliary defects. **a-d** RPE-1 cells were transfected with control or OGA siRNAs and serum-starved for 24 hr. Cells were lysed and immunoblotted (**a**) or subjected to immunofluorescence microscopy (**b**). The percentage of ciliated cells (**c**, n = 100) and ciliary length (**d**, n = 30) were quantified. **e-h** RPE-1 cells were serum-starved and treated with TMG (5 μ M) or the control vehicle for 24 hr. Cells were lysed and immunoblotted (**e**) or subjected to immunofluorescence microscopy (**f**). The percentage of ciliated cells (**g**, n = 100) and ciliary length (**h**, n = 30) were quantified. **i-l** RPE-1 cells were transfected with control or OGT siRNAs and serum-starved for 24 hr. Cells were lysed and immunoblotted (**i**) or subjected to immunofluorescence microscopy (**j**). The percentage of ciliated cells (**k**, n = 100) and ciliary length (**l**, n = 30) were quantified. **m-p** RPE-1 cells were serum-starved and treated with BZX (150 μ M) or the control vehicle for 24 hr. Cells were lysed and immunoblotted (**m**) or subjected to immunofluorescence microscopy (**n**). The percentage of ciliated cells (**o**, n = 100) and ciliary length (**p**, n = 30) were quantified. Scale bars, 10 μ m. *P < 0.05, **P < 0.01, ***P < 0.001, ****P < 0.0001. Error bars indicate SEM.

Supplementary information, Figure S4

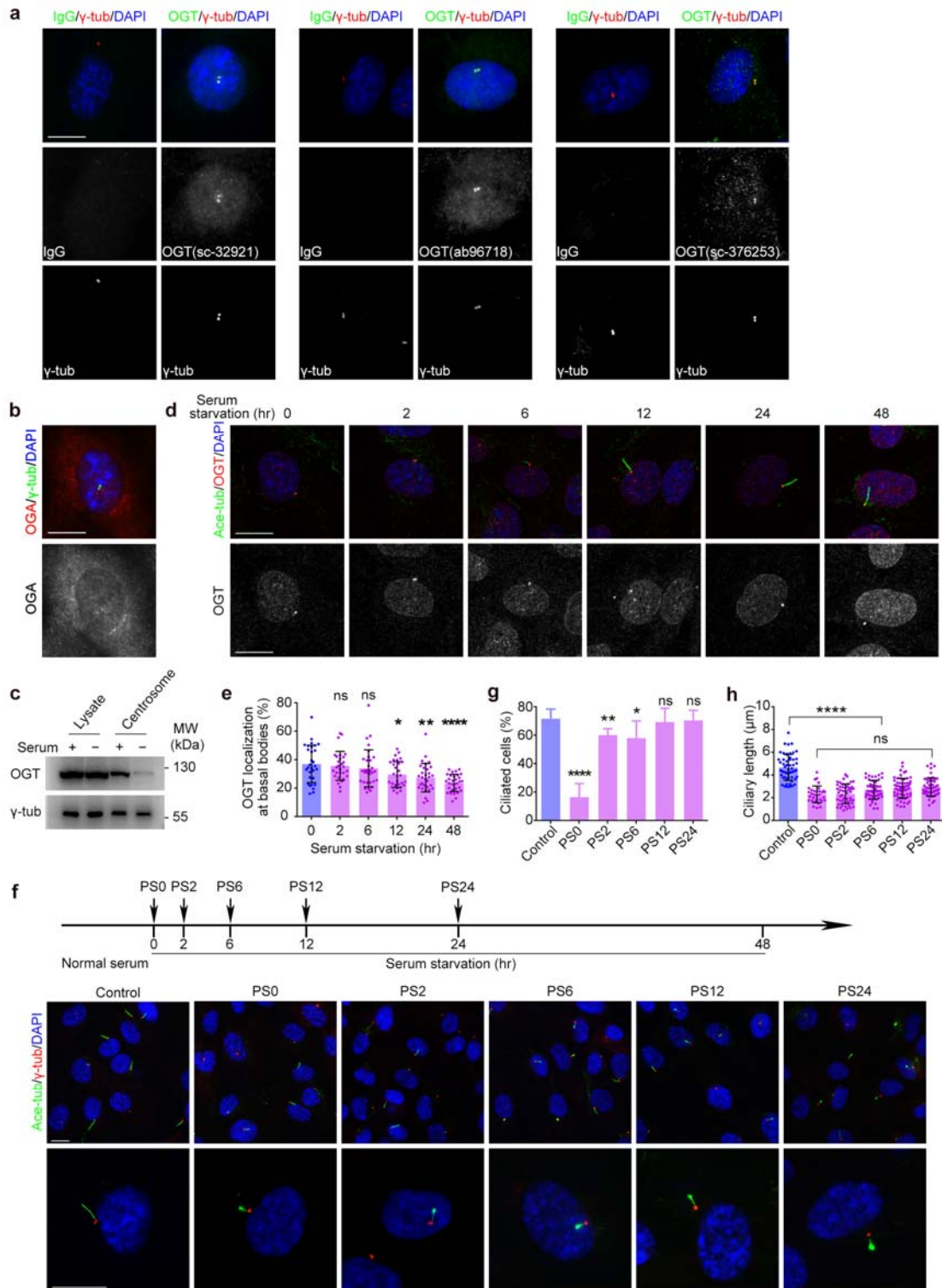


Fig. S4 OGT localization at the basal body/centrosome peaks at the early stages of ciliogenesis. **a** RPE-1 cells were subjected to immunofluorescence microscopy with OGT and γ -tubulin antibodies and DAPI. Three different OGT antibodies and their control IgGs were used. **b** RPE-1 cells were subjected to immunofluorescence microscopy with OGA and γ -tubulin antibodies and DAPI. **c** RPE-1 cells were cultured in media with or without serum for 24 hr, and the lysates or isolated centrosomes were subjected to immunoblotting. **d, e** RPE-1 cells were serum-starved for the indicated time and subjected to immunofluorescence microscopy (**d**). The localization of OGT at the basal body was then quantified (**e**). **f-h** RPE-1 cells were serum-starved for 48 hr, and BZX (150 μ M) was added to the medium at set intervals after serum starvation (PS0, BZX added at initiation of serum starvation; PS2, BZX added after 2 hr of serum starvation; etc.). Cells were subjected to immunofluorescence microscopy (**f**), and the percentage of ciliated cells (**g**, $n = 100$) and ciliary length (**h**, $n = 30$) were quantified. Scale bars, 10 μ m. * $P < 0.05$, ** $P < 0.01$, **** $P < 0.0001$; ns, not significant. Error bars indicate SEM.

Supplementary information, Figure S5

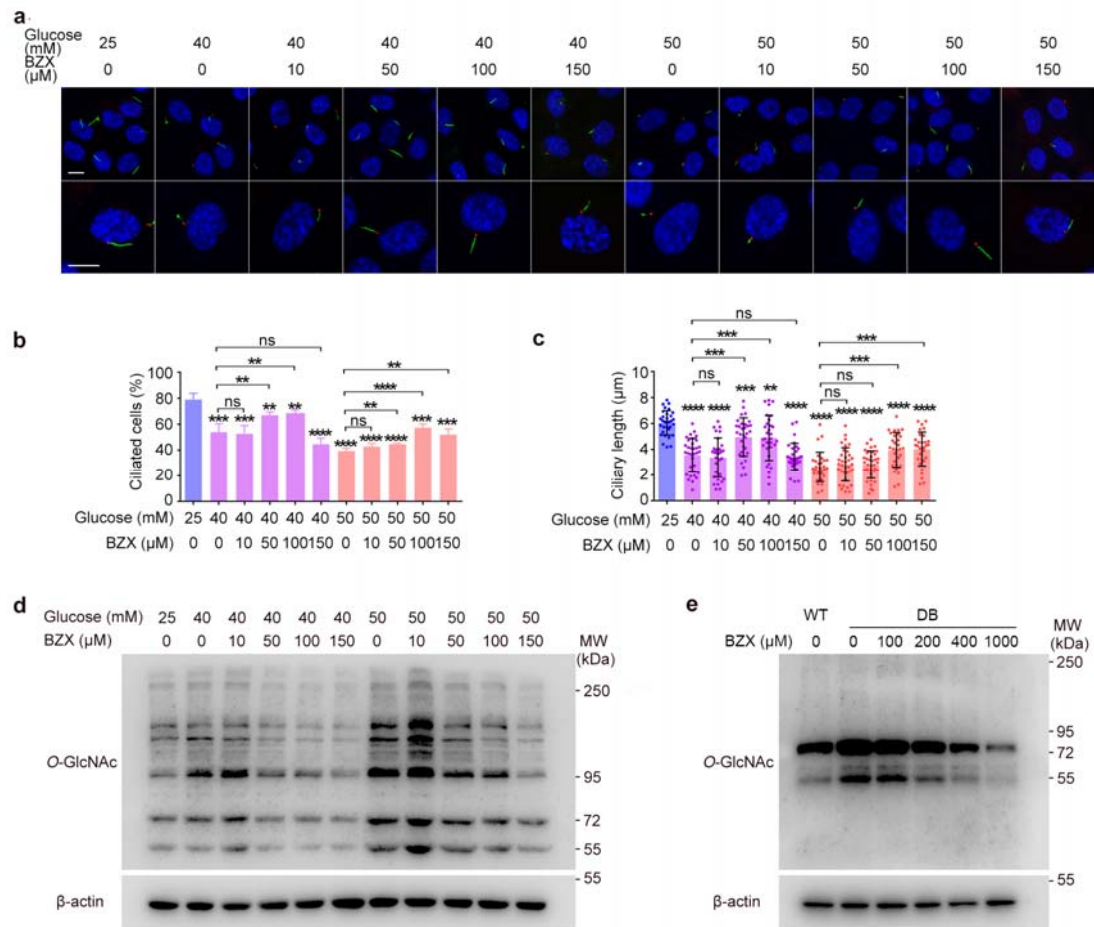


Fig. S5 High glucose-induced ciliary defects could be partially rescued by proper control of protein *O*-GlcNAcylation level. **a-d** RPE-1 cells were cultured in serum-free medium containing the indicated concentrations of glucose and BZX for 48 hr. Cells were subjected to immunofluorescence microscopy (**a**). The percentage of ciliated cells (**b**, $n = 100$) and ciliary length (**c**, $n = 30$) were quantified, and cell lysates were immunoblotted (**d**). **e** WT or DB mice were treated with the indicated doses of BZX for 15 days, and the eye lysates were immunoblotted. Scale bars, 10 μ m. ** $P < 0.01$, *** $P < 0.001$, **** $P < 0.0001$; ns, not significant. Error bars indicate SEM.

Supplementary information, Figure S6

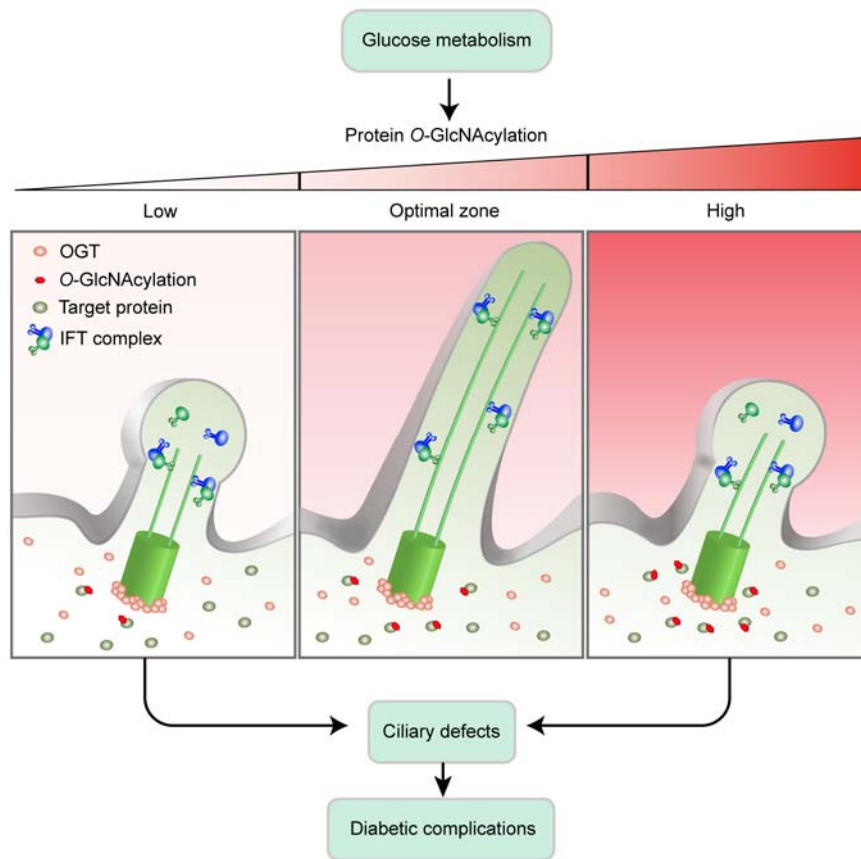


Fig. S6 Model for the function of *O*-GlcNAcylation-dependent ciliary defects in diabetic complications.